Biomaterials Science

ROYAL SOCIETY OF CHEMISTRY

PAPER

View Article Online
View Journal | View Issue

Cite this: *Biomater. Sci.*, 2025, **13**, 6446

A proof-of-concept study on an injectable artificial ovary using a xenogeneic ECM for fertility restoration

Chungmo Yang, †[a,d] Nanum Chung, †[a,b] Chaeyoung Song, †[a,b] Hyerim Kim, [d] Jungwoo Shin, [a,b] Kangwon Lee *[e,f] and Jung Ryeol Lee *[a,b,c]

The development of artificial ovaries presents a promising strategy for patients facing infertility due to chemotherapy or high metastatic potential cancers, where conventional ovarian tissue transplantation poses significant risks. Our study introduces an "injectable artificial ovary" leveraging a xenogeneic extracellular matrix (ECM) hydrogel derived from bovine ovarian tissue. The ECM hydrogel obtained from bovine ovaries and prepared through decellularization, milling, and digestion is injectable and thermoresponsive, preserving the matrix structure without cytotoxicity. This innovative approach delivers a non-surgical alternative for fertility preservation by harnessing the bioactive and adaptable properties of ECM hydrogels to support ovarian follicle maturation and restore endocrine functions. In our results, the hydrogel demonstrated temperature-responsive gelation and biocompatibility, promoting follicle development and increasing 17β-estradiol secretion. Such advancements highlight the potential of this technique to redefine fertility treatments and regenerative medicine. Notably, the *in situ* development of ovarian follicles within the injected hydrogel led to successful ovulation after subcutaneous implantation. Although our study did not demonstrate oocyte maturation and fertilization, our findings suggest that this approach could serve as a heterotopic artificial ovary, offering a promising solution for fertility preservation in patients with high metastasis risk cancers who cannot undergo conventional treatments. This strategy advances artificial ovary technologies, presenting new possibilities for reproductive health and fertility preservation interventions.

Received 2nd July 2025,
Accepted 23rd September 2025

DOI: 10.1039/d5bm01010a

rsc.li/biomaterials-science

Introduction

With an increasing cancer survival rate, the incidence of infertility is a common social issue in patients after chemotherapy.[1] While ovarian tissue transplantation (OTT) of frozen/thawed tissue is a viable technique, it requires ovarian tissue cryopreservation (OTC) as a prerequisite.[2] For patients with high metastatic potential cancers, conventional OTT poses recurrence risks, rendering it non-viable. The use of artificial ovaries represents a promising future approach currently under development. They are not yet an established or experimental clinical service but hold significant potential as an alternative for patients unable to undergo ovarian tissue transplantation due to high metastasis risks. Alternative ways of transplantation have been researched, such as *in vitro* follicle culture and the construction of artificial ovaries.[3] Despite the potential of *in vitro* follicle culture to achieve alternative "oocyte maturation" without recurrence concerns, it faces limitations, including the challenge of sourcing suitable materials for a three-dimensional environment, a low fertility success rate, and technical complexities in the laboratory. Similarly, constructing artificial ovaries is still an unknown realm, even though some research groups have developed ovarian tissue constructs to restore endocrine functions.[4] Several reports have detailed live births resulting from biomaterial-based constructs resembling artificial ovaries in mice. These experi-

[a]*Department of Obstetrics and Gynecology, Seoul National University Bundang Hospital, Seongnam 13620, Republic of Korea. E-mail: leejrmd@snu.ac.kr*
[b]*Department of Translational Medicine, Seoul National University College of Medicine, Seoul 03080, Republic of Korea*
[c]*Department of Obstetrics and Gynecology, Seoul National University College of Medicine, Seoul 03080, Republic of Korea*
[d]*Program in Nanoscience and Technology, Graduate School of Convergence Science and Technology, Seoul National University, Seoul 08826, Republic of Korea*
[e]*Department of Applied Bioengineering, Graduate School of Convergence Science and Technology, Seoul National University, Seoul 08826, Republic of Korea. E-mail: Kangwonlee@snu.ac.kr*
[f]*Research Institute for Convergence Science, Seoul National University, Seoul 08826, South Korea*
†These authors contributed equally to this study.

ments typically involved either isolated follicles or entire ovarian tissue encapsulated in a plasma clot or similar fibrin hydrogel containing growth factors or refined vascular endothelial growth factor components.[5–8] These outcomes show promising potential and underscore the importance of graft vascularization for achieving complete organ function restoration with isolated follicles in biomaterial settings.[5,6] While prior studies have made significant progress in addressing challenges related to artificial ovary development, such as vascularization and structural design, certain limitations remain. Our study aims to build on these advancements by introducing an injectable artificial ovary, which eliminates the need for surgical implantation and leverages transvaginal injection methods commonly used in clinical oocyte retrieval.[9,10]

Artificial organ development encompasses various approaches.[11,12] While electronic devices, such as artificial hearts and prosthetic limbs, have been commercialized, their relevance to tissue-based organ engineering, such as artificial ovaries, is limited. Instead, tissue engineering focuses on constructing biological structures with cells, bioactive molecules, and scaffolds to restore or replace organ function. The tissue engineering approach involves constructing tissues with cells, bioactive molecules, and scaffolds.[13,14] For example, hydrogels have been used for the regeneration of specific tissues and functions with a counterpart cell type or stem cells together with growth factors. The term "organoid" refers to a cell complex with specific functions cultured from cell levels to miniature organ levels *in vitro* as a part of tissue engineering.

A hydrogel is a network of polymers that can capture water in their structures. With the sol–gel transition caused by thermo-, pH, light, and other sources, injectable hydrogels are promising materials for local treatment without an incision in regenerative medicine and tissue engineering.[15] Stimuli-responsive hydrogels are appropriate for use in an injection of cells or biomolecules. Pluronic F127 (F127) gels, one of the thermo-responsive materials, have been extensively studied in the scientific literature for their use as carriers for cells and drugs.[16,17] This interest is due to their minimal toxicity, capability for reverse thermal gelation, high capacity for drug loading, and their ability to form gels under physiological conditions at relatively low concentrations.[18,19] The injectable hydrogels are used in cartilage, bone, or adipose tissue regeneration on defective parts.[20,21] Also, drug-releasing injectable hydrogels are developed for recruiting cells, cancer treatment, and other purposes.[22] One challenge associated with synthetic polymers, such as Poloxamer 407 (F127), is their limited capacity to provide long-term structural support post-injection. To overcome this, F127 is often used as a sacrificial matrix to create porosity or provide space for host cells when combined with ECM hydrogels, which offer significant bioactivity and compatibility advantages.

Extracellular matrix (ECM) hydrogels present significant advantages in tissue engineering due to their bioactive nature and resemblance to native tissues. They create a supportive environment for cell adhesion, growth, and differentiation, facilitated by bioactive molecules such as growth factors and glycoproteins. ECM hydrogels are designed to biodegrade gradually, ensuring smooth integration with the host tissue while avoiding chronic inflammation or immune responses. The mechanical characteristics and bioactivity of ECM hydrogels are highly adaptable, with adjustments possible through the concentration of ECM components or the use of cross-linking agents. This allows for precise customization to meet the specific demands of various tissue engineering applications. The inherent porosity of these hydrogels enhances the diffusion of nutrients and oxygen, supports cell viability and function, and aids in the elimination of metabolic waste. Moreover, ECM hydrogels foster a regenerative microenvironment, promoting the recruitment and differentiation of progenitor cells as well as the formation of new blood vessels, which are crucial for effective tissue repair and regeneration. These properties make ECM hydrogels an essential tool in tissue engineering, with significant potential for advancing therapeutic strategies.[23]

Herein, we present an injectable artificial ovary concept designed to restore reproductive function through heterotopic transplantation (Fig. 1). The platform utilizes a novel, tissue-specific scaffold of a decellularized bovine ovarian extracellular matrix (OECM), which preserves essential native proteins like collagen, fibronectin, and laminin. This distinguishes it from prior synthetic or non-ovarian scaffolds and provides a native-like microenvironment to support transplanted follicles. We confirmed that the OECM has temperature-responsive gelation properties, is free of DNA, and shows no cytotoxicity *in vitro*. The OECM hydrogel provides an appropriate environment for mouse ovarian follicles *in vivo*. Notably, we observed the development of follicles and corpus luteum-like tissue, accompanied by elevated 17β-estradiol (E2) secretion, upon injecting OECM hydrogels with ovarian follicles. Therefore, the proposed method is promising for artificial ovary development through the facile injection of hydrogels containing isolated ovarian follicles.

Results

Decellularization and characterization of OECM hydrogels

Decellularization was to remove the resident cells maintaining tissue extracellular matrix structures. We optimized decellularization protocols and conventional methods in previous studies with minor modifications.[24–26] After decellularization, the ovarian tissues have no cellular components and maintain the extracellular matrix composition, as shown in Fig. 2. The decellularized ovarian tissue (OECM) was milled and digested using pepsin in an acidic solution. The digested OECM shows sol–gel transition behavior confirmed by inverting test (Fig. 2A). The decellularized tissues were histologically confirmed to lack cellular debris or nuclei, as demonstrated by H&E staining and DAPI imaging (Fig. 2B). Also, the structure of the tissue and decellularized tissue was observed by SEM (Fig. 2C). The decellularized tissue maintained its overall structure but became more porous. In Fig. 2C, the decellularized tissues exhibited lower DNA content than native tissues. In the

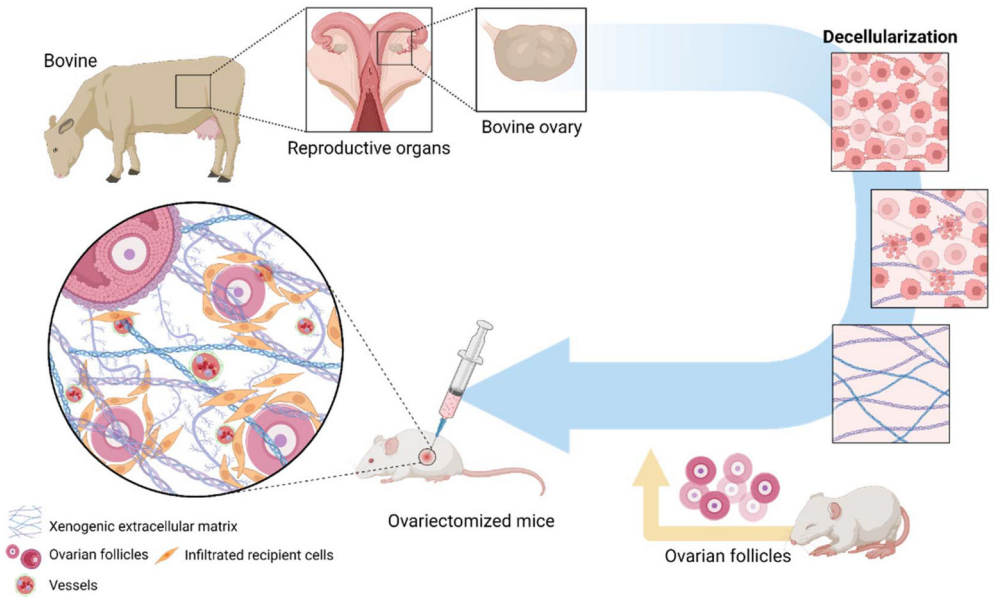

Fig. 1 Schematic illustration of injectable artificial ovary preparation. After harvesting bovine ovaries, decellularization was processed. The thermo-responsive extracellular matrix from the bovine ovary (OECM) was mixed with mouse ovarian follicles and injected to create a xenogeneic artificial ovary.

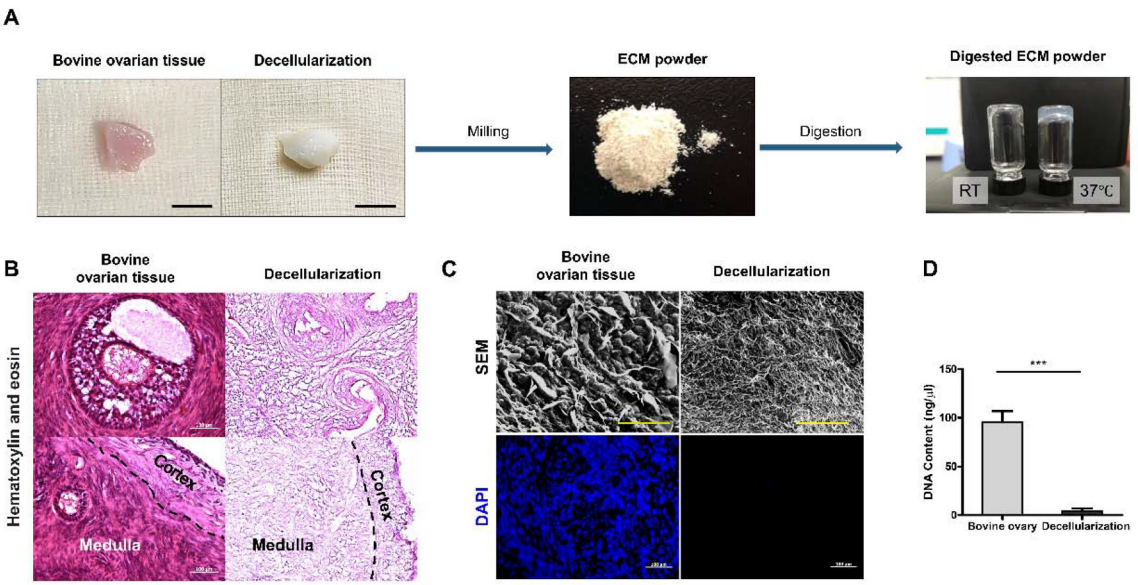

Fig. 2 Decellularization of the bovine ovary. (A) The process of decellularization, milling, and digestion with pepsin. After pepsin digestion, the hydrogel shows gelation properties above room temperature. Scale bar = 1 cm. (B) H&E results from bovine ovarian tissue before and after decellularization, distinguishing between the medulla and cortex parts of the ovary. Scale bar = 100 μm. (C) Images of the scanning electron microscope (SEM) and DAPI staining. Scale bar = 50 μm (in the SEM image) and 100 μm (DAPI staining). (D) Quantification of DNA contents in both bovine ovarian tissue and decellularized tissue (n = 5; ***P < 0.001, data are presented as mean ± SD).

control group and decellularized ovarian tissues, total DNA content was determined to be 95.80 ng μl^{-1} (±10.99) and 4.346 ng μl^{-1} (±2.60), respectively. After decellularization, our decellularized ovarian tissue contained 17.38 ng of DNA per mg of tissue. These results align with established decellularization benchmarks for residual DNA content.[27]

The representative extracellular components remained after removing cells, such as GAGs, collagen, laminin, and fibronectin (Fig. 3A–D). The GAGs and collagen were distributed around ovarian follicles and the ovarian cortex. The cell adhesion proteins laminin and fibronectin were in the whole ovarian tissue and remained prominent throughout the

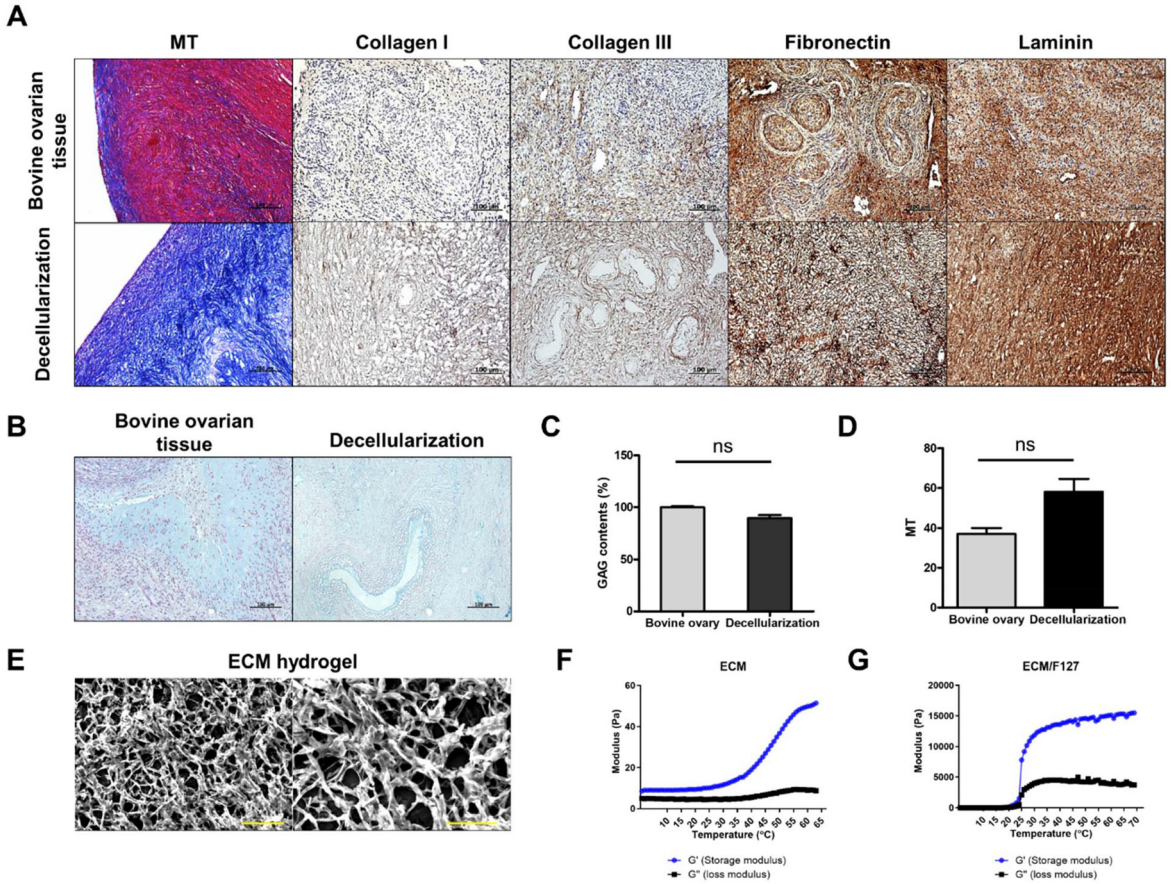

Fig. 3 Characterization of decellularized bovine ovarian tissue. (A) Extracellular matrix components (Masson's trichrome staining and immunohistochemistry of collagens I and III, fibronectin, and laminin) before and after decellularization of bovine ovarian tissue. (B) Alcian blue staining for analysis of glycosaminoglycans (GAGs). Scale bars = 100 μm (A and B). The quantification of GAG and collagen (MT positive area) contents (C and D, n = 3). (E) SEM images of the ECM hydrogel after decellularization, milling, and digestion. Scale bar = 50 μm (left) and 30 μm (right). The mechanical properties of the ECM hydrogel and ECM/F127 hydrogel (F and G). Data are presented as mean ± SD (n = 3 per group).

ovarian tissue post-decellularization. The OECM hydrogels displayed a porous network structure typical of hydrogels (Fig. 3E). The viscoelastic properties of the OECM and OECM-F127 hydrogels were analyzed based on temperature. In the case of the OECM hydrogel, the storage (G') and loss (G'') moduli increase due to gelation at about 35 °C with an increase in temperature. However, the modulus level was relatively low (Fig. 3F). On the other hand, when Pluronic F127 was added to the OECM hydrogel, the storage (G') and loss (G'') moduli increased sharply at about 25 °C (Fig. 3G). The addition of Pluronic F127 was aimed at modifying the physical properties of OECM hydrogels, particularly to lower the gelation temperature and enhance the mechanical rigidity, which are critical for maintaining structural integrity post-injection.

In vitro cytotoxicity of OECM-F127 hydrogels

Live/dead assay results showed that human fibroblasts, 3T3-L1s, and HUVECs cultured on the OECM-F127 surface have no cytotoxicity up to day 3 like the 2D control (Fig. 4A). The cells were alive during experimental periods and proliferated well on the surface of the ECM hydrogel. Additionally, due to the 3D culture, it was possible to observe cells spreading in three dimensions. We investigated cytotoxicity by using leaching solutions after immersion of the OECM-F127 hydrogel in the growth medium for 48 h. In the result of CCK-8 assay by using ECM hydrogel leaching solutions, the cell viability treated with OECM-F127 hydrogel leaching solutions showed no significant difference, which indicated non-toxicity of our hydrogel (Fig. 4B–D).

Development of mouse ovarian follicles in OECM scaffolds after injection

The OECM-F127 hydrogels containing ovarian follicles were directly injected into the subcutis after 4 to 6 weeks after OVX (Fig. 5A). We observed the development of ovarian follicles in the injected OECM-F127 hydrogels through H&E staining, starting from the early secondary stage to the late secondary or antral stage. One day after injection, we found only small pre-antral stage follicles, with no developmental signs. By day 3

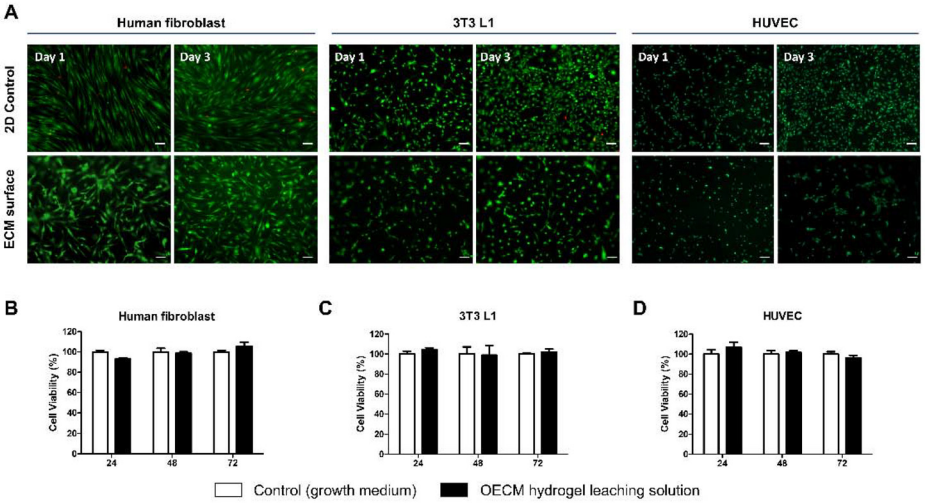

Fig. 4 *In vitro* cytotoxicity of the OECM hydrogel. (A) Fluorescence images of live/dead staining (live cells: green and dead cells: red) of human fibroblasts, mouse fibroblasts (3T3-L1s), and HUVECs. Scale bars = 200 μm. (B–D) Quantified results of CCK-8 cell viability assay after treatment with ECM hydrogel leaching solution (n = 3). Data are presented as mean ± SD (n = 3 per group).

post-injection, the follicles showed an increased number and density of granulosa cells compared to those on day 1. After 1 week, most follicles had developed into early antral follicles. Particularly, corpora lutea-like structures with a hemorrhage were observed within the OECM scaffold after two weeks of injection (Fig. 5B). The injected hydrogel formed a distinct, small, oval-shaped area beneath the skin three weeks after injection. It appeared white and was clearly distinguishable from the surrounding host tissue. The proportion of antral follicles among the total follicles demonstrated a significant increase on days 14 and 21 compared to those at days 1 and 3 (Fig. 5D). Also, Fig. 5E shows the whole structure of the injected OECM scaffold. We can observe the distributed ovarian follicles inside the OECM scaffolds. Interestingly, corpora lutea-like structures were observed within the injected OECM-F127 hydrogel after 14 days (Fig. 5F), randomly distributed throughout the scaffold.

Angiogenesis and proliferative cells in the OECM scaffolds

Angiogenesis plays a crucial role in the growth and survival of ovarian follicles, and ECM hydrogels exhibit strong integration with host tissue, fostering angiogenesis. Our OECM-F127 hydrogels showed significant promotion of angiogenesis after injection and supported the proliferation of cells in ovarian follicles. To confirm endothelial cells sprouting into the hydrogel, the immunohistochemistry of CD31 was carried out. After one day, the CD31 positive area was hardly observed. The CD31-positive area gradually increased during experimental days and was detected around the granulosa cells of the ovarian follicles (Fig. 6A and B). Ki67, a cell proliferation marker, was consistently detected in the granulosa cells and oocytes of most ovarian follicles in the scaffold. There was no significant difference in the Ki67-positive follicle rate between all days (Fig. 6A).

Restoring estradiol levels after OECM hydrogel injection

3 weeks after OVX, the level of estradiol decreased compared to that in normal mice. The estradiol level increased after 3 days post-injection. After 3 days of injection, the estradiol displayed a normal range of concentrations having no statistical difference with normal mice (Fig. 6C). This result suggests a positive impact of the injected OECM-F127 hydrogel containing ovarian follicles on estradiol levels, potentially contributing to the restoration of hormonal balance and response to the hypothalamus–pituitary–ovarian (HPO) axis.

Discussion

This study suggests a concept "injectable ovary" *via* a xenogenic ECM-based injectable hydrogel with ovarian follicles as an artificial ovary for fertility preservation. The ovary-derived ECM includes various components secreted by the cells that make up the ovary, such as stromal cells, granulosa cells, theca cells, and oocytes. The strategic incorporation of Pluronic F127 was critical to our hydrogel's design, where it plays a dual role as both a thermo-responsive agent and a sacrificial matrix. Its thermo-responsive properties facilitate a sol–gel transition at approximately 25 °C, which is ideal for easy injection while ensuring rapid solidification and structural retention at body temperature. More importantly, F127 acts as a sacrificial component *in vivo*. As it dissolves, it creates an interconnected network of micropores within the more stable OECM scaffold. This engineered porosity is crucial for promoting the infiltration of host cells and the formation of new blood vessels (angiogenesis), which is essential for follicle survival. This pro-angiogenic mechanism is strongly supported by our observation of a significant increase in the CD31-positive vascular area over time (Fig. 6). We also used F127 as a sacrificial

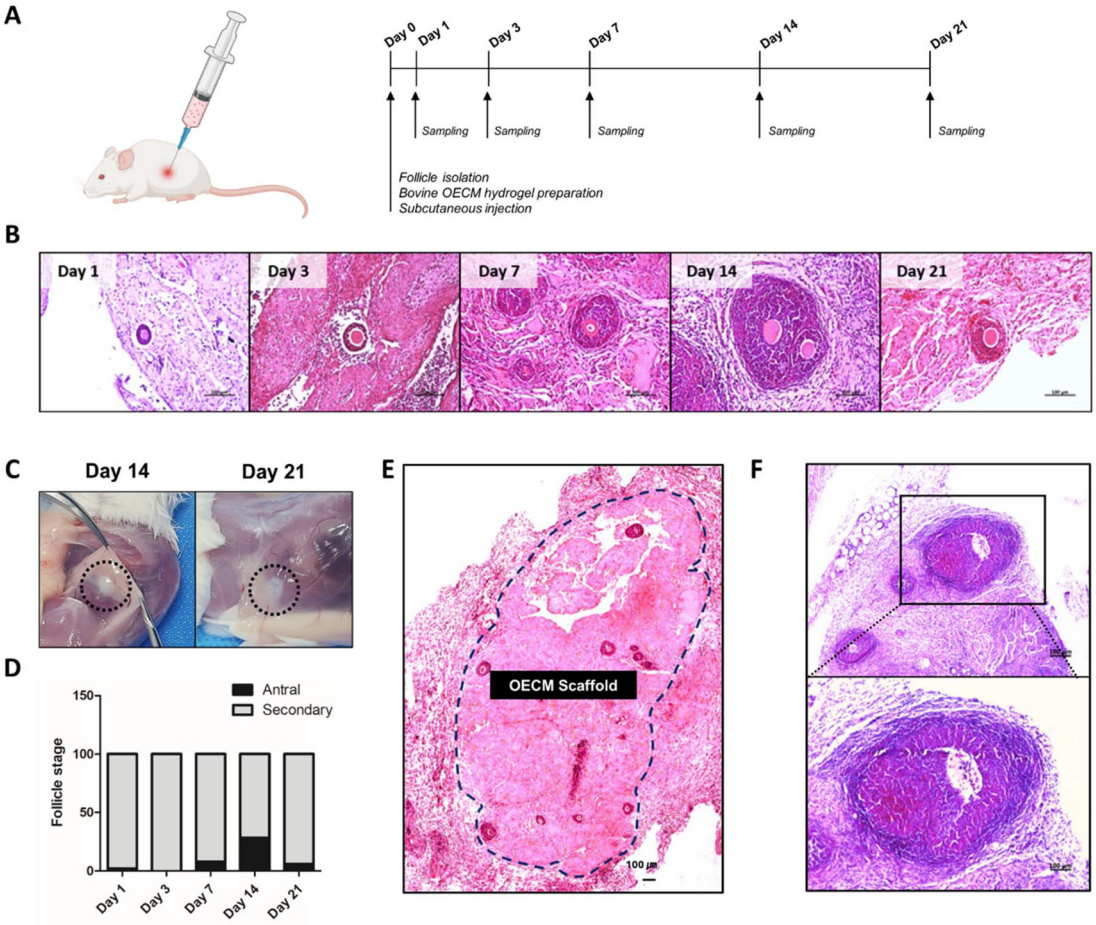

Fig. 5 Injection of the OECM scaffold with mouse ovarian follicles and observation of follicle growth *in vivo*. (A) Experimental scheme. The OECM hydrogel containing follicles was injected subcutaneously into the dorsal area of mice on day 0. Tissues were subsequently retrieved and analyzed on each observation day. (B) Growing follicles in the injected OECM scaffold on each observation day (H&E staining, 200×). (C) Following injection, the OECM scaffold on days 14 and 21 (depicted by black dashed lines). (D) Developmental stages of embedded follicles in OECM scaffolds on each observation day. The embedded follicles displayed 1 or 2 layers of granulosa cells and were approximately 100 μm in diameter at the time of injection. Over time, the follicles advanced to the late secondary and antral stages, marked by continued growth and the presence of an antral cavity (n = 3). (E) The morphology of the whole engrafted OECM scaffold. (F) The corpus lutea-like structure in the engrafted OECM scaffold. All scale bars = 100 μm.

network after injection. We intended that F127 would collapse after injection to maintain the shape of the injected hydrogel and provide pores to facilitate the development of vasculature. This method is widely used for enhancement of angiogenesis toward injected or transplanted hydrogels.[28,29] We investigated a xenogeneic OECM hydrogel (decellularized bovine ovary) applied to mouse ovarian follicles as a supporting matrix and environment. The bovine ovary has high lipid levels in the tissues, and we added lipid removal steps to clarify decellularization. We tried an acetone/ethyl alcohol mixture to remove the lipids in the bovine ovarian tissues successfully. After decellularization, the tissues turned white, confirming the absence of cellular contents. The extracellular matrix structures remained native, as observed by SEM, without cellular contents (Fig. 2c). Furthermore, the biocompatible and thermoresponsive properties of Pluronic F127 ensured that the hydrogel adapted quickly to body temperatures, promoting rapid gelation upon injection, which is crucial for immediate structural support and minimizing the risk of dispersion or dislocation. Notably, decellularized bovine ovarian tissues had about 95% of DNA removed compared to native tissues, whereas the amounts of ECM components including GAGs, collagens I and III, fibronectin, and laminin showed no significant differences from those in native ovarian tissues (Fig. 3). The decellularized tissues were lyophilized, milled, and digested using an acidic pepsin solution to solubilize ECM powder. The neutralized ECM and Pluronic F127 were mixed with ovarian follicles before injection. We intended that Pluronic F127 should have a unique feature: a sol–gel transition with temperature differing from that with the concentration. Since Pluronic F127 can easily be removed *in vivo* environment, the polymer is widely used as a removable supporting material or to create hollow channels or cavities inside hydrogels in tissue engineering applications. Therefore, we

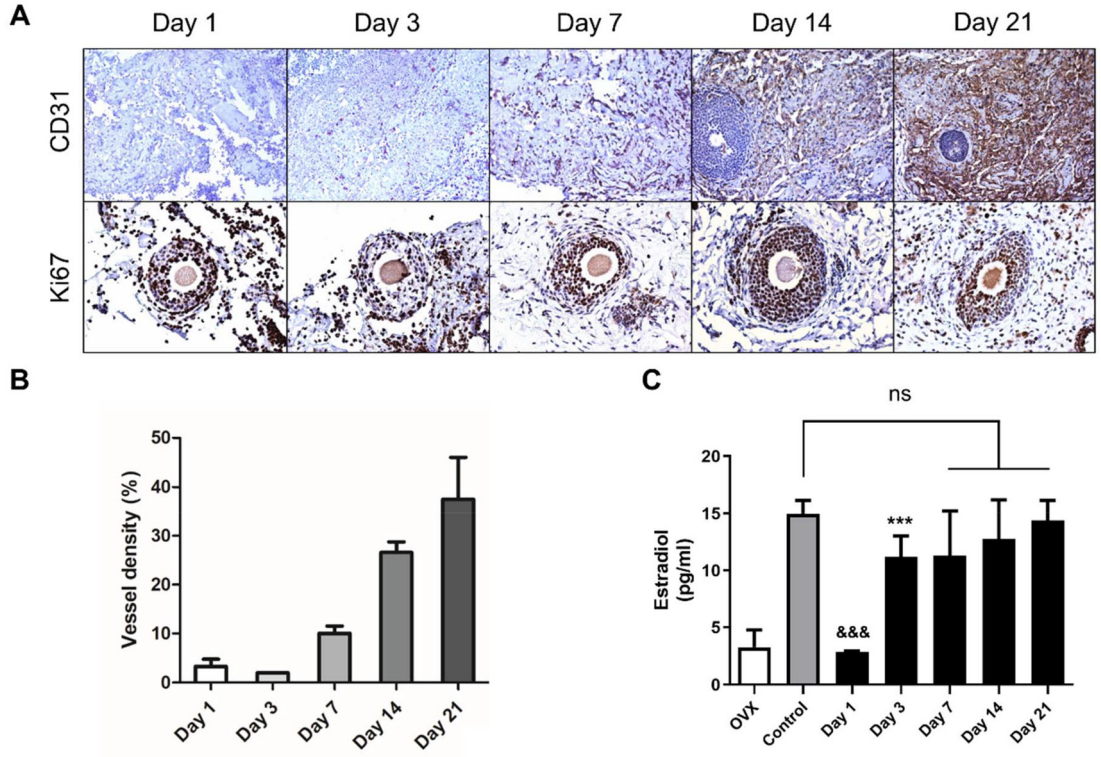

Fig. 6 Immunohistochemistry of the injected OECM scaffold with mouse ovarian follicles. (A) Immunohistochemical staining (brown) for CD31 (angiogenesis marker, 1 : 50) and Ki67 (proliferation marker, 1 : 50). Embedded follicles exhibited progressive follicular development over time, characterized by proliferation of granulosa cells and the presence of an antrum. (B) The quantitative analysis of the CD 31 positive area (n = 3). (C) The serum estradiol levels on each observation day (n = 4). From the 7th day post-engraftment onwards, the levels of estradiol in the serum returned to concentrations comparable to those of normal mice (data are presented as mean ± SEM, ns; non-significant, &&&; compared to control, ***; compared to OVX, $p < 0.001$, one-way ANOVA).

used Pluronic F127 to provide a three-dimensional structure to follicles and injectability to ECM hydrogels.

All the previously reported studies on artificial ovaries are performed through invasive procedures, which can damage the scaffold implantation site and tissues, resulting in the failure of tissue engrafting.[30,31] The published studies on bioengineered artificial ovaries have typically focused on transplantation of dissected ovarian tissues with biomaterials,[6,32] preparation of biomaterials-based constructs for hormone therapy,[33,34] or injection of biomaterials into pre-existing ovaries.[35] In addition, it takes a lot of time due to the process of *in vitro* culture by seeding cells in the ECM scaffold and surgical operations.[36] In this study, we used reproductively compromised mice by complete ovary removal and transplanted the artificial ovary *via* injection to a different location to overcome the existing artificial ovary's limitations and improve the application method. We prepared an artificial ovary for xenotransplantation injection that was manufactured using an ECM obtained from the decellularized bovine ovary with the biomaterial Pluronic F127 and mouse ovarian follicles. The OECM-F127 hydrogel was shown to increase storage (G') and loss (G'') moduli more at a lower temperature than the OECM alone. This helps maintain the shape of the scaffold irrespective of the implantation site and extends the retention time *in vivo*. The combination of the OECM and Pluronic F127 with an established protocol demonstrated no cytotoxicity against several types of cells. The morphology of the embedded follicles survived and developed in the OECM scaffold with the recovery of the serum estrogen level around the normal range (Fig. 5 and 6). The injected OECM-F127 hydrogel facilitated the development of corpora lutea-like structures, as evidenced in Fig. 5. This observation is crucial as it demonstrates that the injected scaffold provides an appropriate microenvironment that supports the embedded follicles in OVX mice. It is important to note that while most studies utilize methods like transplanting ovarian tissue fragments or partially removing the ovary for transplantation, our study took a different approach. Furthermore, it interacts effectively with the hypothalamic–pituitary–ovarian (HPO) axis, suggesting its capability to support natural ovulation processes. The detection of Ki67 in the granulosa cells of the transplanted follicles would be evidence to prove that they had grown and developed in the OECM scaffold. Also, it was confirmed that angiogenesis in the OECM scaffold was normally performed and created healthy vessels through CD31 staining, which is a critical path for hormonal responses and follicle development (Fig. 6).

Given the challenges of obtaining auto-derived tissues, xenotransplantation is emerging as a promising alternative in organ

transplantation.[37,38] Previous attempts to transplant a kidney, liver, or heart have failed because of immune rejection, which is the main issue of organ transplantation.[39,40] In tissue engineering, the scaffolds designed for organ regeneration also address immune responses after transplantation.[41] Decellularized ECM hydrogels are known to exhibit a sufficiently low immune response compared to traditional xenotransplantation,[23] and our findings support this, showing low CD3 detection indicative of minimal T cell infiltration (Fig. S1). The ECM components were introduced to reconstitute the original tissue environment and eliminate immune rejection.[27,42–44] In the ovary, the tissue environment has complications generated by ovarian stroma cells and follicular cells. Furthermore, it is necessary to discuss the limitations inherent to the heterotopic transplantation model used in this study. We selected a subcutaneous site for transplantation due to its easy accessibility for monitoring graft survival and vascularization. This approach is well-suited for initial proof-of-concept studies to evaluate the fundamental viability of a scaffold. However, the subcutaneous environment differs significantly from the native ovarian site (orthotopic) in terms of vascular supply, innervation, and paracrine signalling, which may compromise follicular development and oocyte quality. Critically, heterotopic transplantation does not allow for natural ovulation and oocyte pickup by the fallopian tube, thus necessitating *in vitro* fertilization (IVF) to achieve pregnancy. Future studies should therefore include orthotopic transplantation models to assess the potential of our dECM hydrogel for restoring natural fertility.

We introduce a novel approach that diverges from conventional strategies by utilizing a minimally invasive injectable hydrogel to reconstruct the ovarian environment *in situ* while minimizing immune rejection (Fig. 7). This demonstrates the excellent biocompatibility of our OECM scaffold, which is a critical prerequisite for successful long-term engraftment and function. However, while the scaffold successfully integrated with the host tissue immunologically and supported follicular development and serum estradiol recovery, this study did not provide direct evidence of the ultimate reproductive function: ovulation and oocyte viability. Furthermore, its long-term functional stability was not assessed. It is important to note, however, that the repeatable, minimally invasive nature of our injectable platform offers a flexible clinical strategy that may not require permanent functionality for successful fertility restoration. To address these functional gaps, future studies will build upon this successful engraftment by including oocyte recovery and mating experiments to confirm that the regenerated ovarian environment can produce viable gametes.

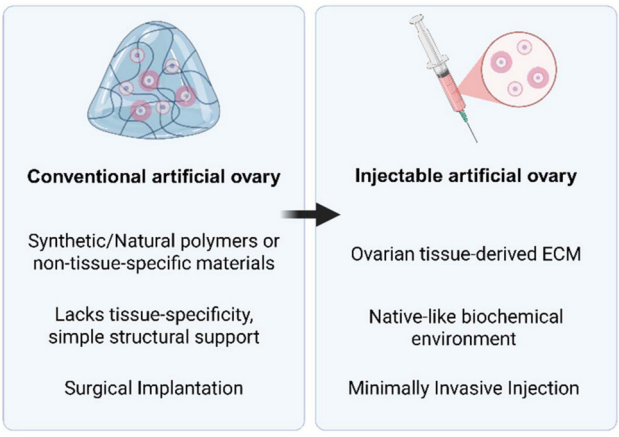

Fig. 7 Comparison of conventional and injectable artificial ovary platforms. The conventional method (left) typically involves surgical implantation of a pre-formed, non-tissue-specific scaffold. Our injectable approach (right) is a minimally invasive alternative that uses an ovarian tissue-derived ECM hydrogel to create a more physiologically relevant microenvironment for follicle support.

Materials and methods

Decellularization of bovine ovaries (OECM)

The cattle (24–36 months old) used in this study were of the Bos taurus coreanae breed and were sourced from a slaughterhouse (Hoengseong KC Co., Ltd, Hoengseong Hanwoo Meat Processing Center, Hoengseong, Republic of Korea). On the morning of the slaughter day, a technician prepared saline solution and a temperature-controlled transport container. Immediately after the ovaries were extracted, they were transported to us *via* a vehicle within three hours. Precise details regarding the breed or estrous phase of the ovaries (luteal *vs.* follicular) were not available. Ovaries were randomly selected and sliced into uniform 1 cm^3 cubical shapes for decellularization. The decellularization method was conducted following the protocol reported, with slight optimization to improve reproducibility.[24,45–47] The dissected tissues were placed in an excess of 0.1% of Triton X-100 on an orbital shaker vigorously. After 24 hours, the solution was replaced with 0.1% sodium dodecyl sulfate (SDS) solution to continue decellularization. The SDS solution used during the decellularization process of bovine ovaries was replaced every 12 hours for a duration of 4 days. To terminate decellularization, the tissue pieces were washed with DPBS for 1 hour. Following the washing steps, the decellularized tissues were dehydrated using graded ethyl alcohol (25% and 50%), 25% acetone/75% ethyl alcohol, and 100% ethyl alcohol to ensure decellularization and removal of lipid content. Subsequently, the dehydrated tissues underwent lyophilization for a period of 5 days and were subjected to five cycles of milling using a freeze mill (SPEX 6875D, SPEX, CA, Costa Mesa, U.S.A.). The resulting decellularized bovine ovary powder (OECM) was stored at −20 °C for further use. Additionally, some pieces of decellularized tissue were fixed in 4% paraformaldehyde (PFA) and embedded in paraffin for histological assessments or prefixed and fixed with 5% osmium tetroxide and 2.5% glutaraldehyde for scanning electron microscopy (SEM) imaging.

Characterization of natural and decellularized ovarian tissue

The PFA-fixed native or decellularized ovarian tissues were embedded in paraffin and subsequently sectioned to a thick-

ness of 4 μm. We conducted H&E staining, DNA content quantification, and DAPI staining to confirm decellularization and optimize the protocol of decellularization. Moreover, alcian blue (glycosaminoglycans (GAGs)) and immunohistochemistry (collagens I and IV, fibronectin, and laminin) provide to maintain the native tissue structure and extracellular matrix contents. The paraformaldehyde-fixed native or decellularized ovarian tissues were embedded in paraffin and sectioned with a thickness of 4 μm.

A scanning electron microscope (SEM; SNE-3200 (SEC, Suwon, Korea)) was used to observe and maintain the tissue structure before or after decellularization processes. For the SEM study, the native or decellularized tissue pieces were fixed with 2.5% glutaraldehyde and 5% osmium tetroxide and air-dried for 1 day. The dried tissue pieces were trimmed using a surgical blade and coated with platinum and then the tissue structure was observed.

Quantity of DNA content

Following the decellularization process, residual DNA content in the tissues was extracted utilizing DNeasy Blood & Tissue Kits (Qiagen, Hilden, Germany) in accordance with the manufacturer's protocols. The DNA yield (ng μL^{-1}) of each sample (25 mg of tissue in 100 μL) was spectrophotometrically quantified in triplicate according to the optical density at γ = 260 nm using a Nanodrop 2000 spectrophotometer (Thermo Fisher Scientific, Waltham, MA, USA).

In vitro cytotoxicity of OECM hydrogels

To identify the cytotoxicity of OECM hydrogels, a live/dead assay was performed on the surface of OECM hydrogels against human fibroblasts, 3T3-L1s, and human umbilical vein endothelial cells (HUVECs). 100 μl of the pH-adjusted pre-gel solution was placed in a 96-well plate and incubated for 30 min in a humidified 37 °C incubator to complete gelation. Then, 5 × 103 cells were seeded on the surface of the hydrogel. The live/dead assay was performed after 24 h and 72 h. A cell counting kit-8 (CCK-8) assay was performed as another technique to verify cytotoxicity. The CCK-8 assay was also performed against human fibroblasts, 3T3-L1s, and Human Umbilical Vein Endothelial Cells (HUVECs). The cell cytotoxicity test was performed using standard Dulbecco's modified Eagle's medium (DMEM) and leaching solution prepared by incubating OECM hydrogels in DMEM for 48 h. The cells were seeded at 5×10^3 cells per well in a 96-well plate for 24 h. Following this, the medium was replaced with either DMEM or hydrogel leaching solutions. CCK-8 solution was added to each well after 1, 2, and 3 days of culture, and the optical density was measured at 450 nm using a microplate reader.

Rheological analysis of OECM and OECM-F127 hydrogels

After decellularization and milling processes, the milled ECM powder was digested in 1 mg mL^{-1} of pepsin in 0.01 N hydrochloric acid (HCl) for a final concentration of 10 mg of ECM per ml. Then, the solution was gently stirred for 48 h and adjusted to neutral pH. Finally, we used 200 mg of F127 in 1 ml of digested OECM solution before mixing with ovarian follicles. The viscoelastic properties of OECM or F127-OECM hydrogels were measured using an MCR302 series rheometer (Anton Paar, Graz, Austria). The strain amplitude was 1%, the frequency was 1 Hz, the heating rate was 1 °C min^{-1}, and the scanning temperature ranged from 15 to 60 °C. The OECM-F127 mixture was prepared by dissolving Pluronic F127, which enhances the mechanical stability and injectability of hydrogels, in a cold OECM solution at a concentration optimal for achieving rapid gelation at physiological temperatures (approximately 25 °C), facilitating *in situ* formation when injected.

Isolation of mouse follicles and subcutaneous injection of the OECM-F127/ovarian follicle hydrogel

Animal experimental procedures in this study were conducted with the approval of the Institutional Animal Care and Use Committee (IACUC) of Seoul National University Bundang Hospital (Approval number: BA-2002-291-020-06). All mice were bred and housed in a controlled setting under specific pathogen-free (SPF) conditions. The conditions included regulated temperature and humidity and a 12-hour cycle of light and darkness, and they received food and water *ad libitum*. Isolation of mouse ovarian follicles was conducted by mechanically puncturing ovaries from 10–14 day-old postnatal ICR female mice (Orient Co., Seongnam, South Korea) as described elsewhere.[24] In brief, the ovaries from the sacrificed mice were transported in a follicle puncture medium (alpha-MEM supplemented with 10% fetal bovine serum [FBS] and 1% penicillin–streptomycin [PS]) and the ovaries were punctured mechanically using 31G needles, under a microscope. After washing the isolated follicles, only those with a diameter of 100–120 μm were sorted. A total of 100 ovarian follicles were mixed into the OECM/F127 hydrogel (200 mg of F127 per ml of digested ECM) per 100 μl volume on ice. The hydrogel–follicle mixture was loaded into a BD® Single Use Syringe, Luer-Lock Type (Becton, Dickinson and Company, US) with a 21G needle. 100 μl of OECM-F127 hydrogel containing ovarian follicles was injected carefully into the dorsal subcutis of anesthetized ICR mice (12 to 13 weeks old, 4 to 6 weeks after ovariectomy (OVX)) with temperature regulation on a warm plate. The injected OECM-F127 hydrogel scaffolds and whole blood were collected post-injection on days 1, 3, 7, 14, and 21. In this study, one or two individuals of 2-weeks-old female mice as follicle donors and used 5 mice per group. The scaffold samples were fixed for the histological analysis, and the whole blood was centrifuged at 14 000 rpm for 15 minutes at 4 °C, and then only serum was separated and stored at −20 °C until hormone level analysis.

Histological analysis of ovarian follicles in the injected hydrogel

H&E staining was performed to confirm the transplanted follicles' morphology and growth. The proportion of antral follicles among all follicles was counted to confirm the develop-

ment of follicles within the OECM scaffold. Deparaffinized and rehydrated tissue sections were treated with hematoxylin for 1 minute. After rinsing in running tap water, the samples were dipped in 1% hydrochloric acid (HCl) in 70% ethanol 3 times for 2 seconds and then they were dipped in eosin for 20 seconds and rinsed. The slides were mounted with a mounting medium (Dako, Copenhagen, Denmark). We selected follicles measuring 100–120 μm in diameter, which corresponds to the early secondary stage of development. We used the same classification of ovarian follicles' developmental stages from the previous studies: primordial (single layer of flattened pre-granulosa cells), primary (single-layer granulosa cells [GC] including cuboidal forms), secondary (at least two layers of cuboidal GC), and antral (multiple layers of cuboidal GC with an antrum).[48,49] The integrity of each follicle was evaluated using the following criteria outlined in a previous study: G1 (good: intact spherical follicles and oocytes), G2 (fair: GC pulled away from the edge of follicles but with intact oocytes), and G3 (poor: disruption and loss of granulosa and theca cells, pyknotic nuclei, and missing oocytes).

Serum hormone levels

The serum was retrieved from whole blood using cardiac puncture. We analyzed 17β-estradiol (E2) levels to evaluate ovarian function after transplantation. The hormone levels were measured using an enzyme-linked immunosorbent assay (ELISA) (Mouse/Rat Estradiol, Calbiotech, El Cajon, CA, USA), according to the manufacturer's protocols.

Immunohistochemical analysis for vessel density and cellular proliferation

To investigate the formation of blood vessels and angiogenesis in the OECM scaffold, CD31, an endothelial cell marker, was stained using an anti-CD31 antibody. Also, Ki67 was employed to confirm the proliferation of follicles. The unstained slides were deparaffinized and rehydrated in xylene and ethanol, respectively. The target antigen retrieval solution (pH 6.0, citrate buffer) was treated for 20 min in a microwave. The sections were treated with peroxidase blocking solution (Dako, Copenhagen, Denmark) for 10 min, followed by incubation with an anti-CD31 (or Ki67) antibody (1 : 50 dilution; Abcam, Cambridge, MA, USA) overnight at 4 °C. After washing, the sections were treated with EnVision + HRP (Dako, Copenhagen, Denmark) for 1 h and subsequently with Liquid DAB + Substrate (Dako, Copenhagen, Denmark) for 10 min at room temperature (RT, 25 °C) followed by counterstaining with hematoxylin. The slides were mounted with a mounting medium (Dako, Copenhagen, Denmark), and the CD31 or Ki67 (+) area was measured using ImageJ software (National Institutes of Health, Bethesda, MD, USA) under a light microscope at ×100 magnification.

Statistical analysis

Statistical analysis and graph preparation were carried out using GraphPad Prism version 10.0.0 software (California, San Diego). For the quantified data of the DNA and GAG contents, the number of follicles, and CD31 staining, one-way analysis of variances (ANOVA) and Tukey's multiple comparison tests were performed. All graphs were generated based on the mean ± standard deviation (SD), and the criteria for determining statistically significant differences were set as $*p < 0.05$, $** p < 0.01$, and $*** p < 0.001$.

Conclusions

In this study, we report a novel approach for the development of an "injectable artificial ovary" utilizing a xenogeneic ECM-based tissue engineering strategy. Our perspectives suggest the feasibility of the development of functional organ ectopic regions with preserved ovarian follicles *via* a new methodology. This study utilized an ovarian ECM obtained from a bovine ovary, which facilitated the construction of tissue through *in situ* injection. From our results, we demonstrated that a decellularized OECM hydrogel facilitates tissue regeneration and development with ovarian follicles after injection. Notably, we observed corpora lutea, implying successful ovulation in the injected OECM hydrogel. Furthermore, histological analysis revealed the integration of the injected OECM hydrogel with host tissues, highlighting its compatibility and potential for long-term functionality. This study represents a proof-of-concept toward the development of an effective method for preparing artificial ovaries for advanced reproductive therapies. We acknowledge that the subcutaneous implantation in this study represents a heterotopic site, which is less physiologically representative than an orthotopic location. This approach was intentionally chosen for this proof-of-concept investigation as it allowed for straightforward monitoring and retrieval of the injected scaffold. While this model limits the potential for natural conception, heterotopic transplantation has clinical relevance for fertility preservation strategies coupled with *in vitro* fertilization.

A significant advantage of our platform is its injectable nature, which avoids the need for invasive surgical implantation. This feature is critical for future clinical translation, as it would allow for minimally invasive delivery into more physiologically relevant sites. In conclusion, the developed technique for injectable ovaries is promising for constructing an artificial ovary by supporting follicular growth and restoring endocrine function. While direct evidence of fertility restoration has not yet been demonstrated, this study provides a strong foundation for future translational research in ovarian tissue engineering.

Author contributions

According to the CRediT contributorship taxonomy, CY and CS performed conceptualization, data curation, formal analysis, methodology, validation, visualization, writing – original draft, and writing – review and editing. NC performed data curation, methodology, validation, visualization, writing – original draft,

and writing – review and editing. HK performed data curation, methodology, and visualization. JS performed data curation, methodology, and visualization. KL and JRL performed conceptualization, funding acquisition, validation, writing – original draft, and writing – review and editing.

Conflicts of interest

There are no conflicts to declare.

Ethical statement

All animal procedures were performed in accordance with the Guidelines for Care and Use of Laboratory Animals of Seoul National University and approved by the Animal Ethics Committee of Seoul National University Bundang Hospital (Approval number: BA-2002-291-020-06).

Data availability

The data supporting this article have been included as part of the supplementary information (SI). Supplementary information is available. See DOI: https://doi.org/10.1039/d5bm01010a.

Acknowledgements

This research was supported by a grant from the Korea Health Technology R&D Project through the Korea Health Industry Development Institute (KHIDI), funded by the Ministry of Health & Welfare, Republic of Korea (grant number: HI22C1394), and was supported by grant no. 14-2020-007 from the SNUBH Research Fund.

References

1 M. P. Velez, H. Richardson, N. N. Baxter, C. McClintock, E. Greenblatt, R. Barr and M. Green, *Hum. Reprod.*, 2021, **36**, 1981–1988.
2 S. Y. Kim, S. K. Kim, J. R. Lee and T. K. Woodruff, *J. Gynecol. Oncol.*, 2016, **27**, e22.
3 C. A. Amorim and A. Shikanov, *Future Oncol.*, 2016, **12**, 2323–2332.
4 X. Peng, C. Cheng, X. Zhang, X. He and Y. Liu, *Ann. Biomed. Eng.*, 2023, **51**, 461–478.
5 A. Shikanov, Z. Zhang, M. Xu, R. M. Smith, A. Rajan, T. K. Woodruff and L. D. Shea, *Tissue Eng., Part A*, 2011, **17**, 3095–3104.
6 E. Kniazeva, A. N. Hardy, S. A. Boukaidi, T. K. Woodruff, J. S. Jeruss and L. D. Shea, *Sci. Rep.*, 2015, **5**, 17709.
7 J. Carroll and R. G. Gosden, *Hum. Reprod.*, 1993, **8**, 1163–1167.
8 R. G. Gosden, *Hum. Reprod.*, 1990, **5**, 499–504.
9 M. M. Laronda, A. E. Jakus, K. A. Whelan, J. A. Wertheim, R. N. Shah and T. K. Woodruff, *Biomaterials*, 2015, **50**, 20–29.
10 C. D. Wood, M. Vijayvergia, F. H. Miller, T. Carroll, C. Fasanati, L. D. Shea, L. C. Brinson and T. K. Woodruff, *Acta Biomater.*, 2015, **13**, 295–300.
11 X. Wang, *Cell Transplant.*, 2019, **28**, 5–17.
12 A. Hitzmann, H. Masuda, S. Ikemoto and K. Hosoda, *Adv. Rob.*, 2018, **32**, 865–878.
13 A. Jordan and V. Tchantchaleishvili, *Artif. Organs*, 2020, **44**, 1318–1319.
14 T. K. Rajab, T. J. O'Malley and V. Tchantchaleishvili, *Artif. Organs*, 2020, **44**, 1031–1043.
15 S. Saska, L. Pilatti, A. Blay and J. A. Shibli, *Polymers*, 2021, **13**(11), 1685.
16 J. C. Gilbert, J. Hadgraft, A. Bye and L. G. Brookes, *Int. J. Pharm.*, 1986, **32**, 223–228.
17 Y. Yang, J. Wang, X. Zhang, W. Lu and Q. Zhang, *J. Controlled Release*, 2009, **135**, 175–182.
18 J. M. Brunet-Maheu, J. C. Fernandes, C. A. de Lacerda, Q. Shi, M. Benderdour and P. Lavigne, *J. Biomater. Appl.*, 2009, **24**, 275–287.
19 S. F. Khattak, S. R. Bhatia and S. C. Roberts, *Tissue Eng.*, 2005, **11**, 974–983.
20 S. Bordbar, N. Lotfi Bakhshaiesh, M. Khanmohammadi, F. A. Sayahpour, M. Alini and M. Baghaban Eslaminejad, *J. Biomed. Mater. Res., Part A*, 2020, **108**, 938–946.
21 X. Li, S. A. Q. Xu, F. Alshehri, M. Zeng, D. Zhou, J. Li, G. Zhou and W. Wang, *ACS Appl. Bio Mater.*, 2020, **3**, 4756–4765.
22 J.-A. Yang, J. Yeom, B. W. Hwang, A. S. Hoffman and S. K. Hahn, *Prog. Polym. Sci.*, 2014, **39**, 1973–1986.
23 L. T. Saldin, M. C. Cramer, S. S. Velankar, L. J. White and S. F. Badylak, *Acta Biomater.*, 2017, **49**, 1–15.
24 A. E. Jakus, M. M. Laronda, A. S. Rashedi, C. M. Robinson, C. Lee, S. W. Jordan, K. E. Orwig, T. K. Woodruff and R. N. Shah, *Adv. Funct. Mater.*, 2017, **27**(34), 1700992.
25 N. F. Henning, R. D. LeDuc, K. A. Even and M. M. Laronda, *Sci. Rep.*, 2019, **9**, 20001.
26 D. A. Young, D. O. Ibrahim, D. Hu and K. L. Christman, *Acta Biomater.*, 2011, **7**, 1040–1049.
27 P. M. Crapo, T. W. Gilbert and S. F. Badylak, *Biomaterials*, 2011, **32**, 3233–3243.
28 B. Pan, L. Shao, J. Jiang, S. Zou, H. Kong, R. Hou, Y. Yao, J. Du and Y. Jin, *Mater. Des.*, 2022, **222**, 111012.
29 Z. Wang, C. Huang, X. Han, S. Li, Z. Wang, J. Huang, H. Liu and Z. Chen, *Mater. Des.*, 2022, **217**, 110662.
30 E. Cho, Y. Y. Kim, K. Noh and S. Y. Ku, *J. Tissue Eng. Regener. Med.*, 2019, **13**, 1294–1315.
31 M. M. Laronda, A. L. Rutz, S. Xiao, K. A. Whelan, F. E. Duncan, E. W. Roth, T. K. Woodruff and R. N. Shah, *Nat. Commun.*, 2017, **8**, 15261.
32 J. Kim, A. S. Perez, J. Claflin, A. David, H. Zhou and A. Shikanov, *npj Regener. Med.*, 2016, **1**, 16010.
33 S. Sittadjody, J. M. Saul, J. P. McQuilling, S. Joo, T. C. Register, J. J. Yoo, A. Atala and E. C. Opara, *Nat. Commun.*, 2017, **8**, 1858.

34 H.-J. Yoon, Y. J. Lee, S. Baek, Y. S. Chung, D.-H. Kim, J. H. Lee, Y. C. Shin, Y. M. Shin, C. Ryu, H.-S. Kim, S. H. Ahn, H. Kim, Y. B. Won, I. Lee, M. J. Jeon, S. H. Cho, B. S. Lee, H.-J. Sung and Y. S. Choi, *Sci. Adv.*, 2021, **7**, eabe8873.
35 M. J. Buckenmeyer, M. Sukhwani, A. Iftikhar, A. L. Nolfi, Z. Xian, S. Dadi, Z. W. Case, S. R. Steimer, A. D'Amore, K. E. Orwig and B. N. Brown, *J. Tissue Eng.*, 2023, **14**, 20417314231197282.
36 G. Pennarossa, T. De Iorio, F. Gandolfi and T. A. L. Brevini, *Cells*, 2021, **10**(8), 2126.
37 Y.-G. Yang and M. Sykes, *Nat. Rev. Immunol.*, 2007, **7**, 519–531.
38 B. Ekser, M. Ezzelarab, H. Hara, D. J. van der Windt, M. Wijkstrom, R. Bottino, M. Trucco and D. K. C. Cooper, *Lancet*, 2012, **379**, 672–683.
39 T. Lu, B. Yang, R. Wang and C. Qin, *Front. Immunol.*, 2019, **10**, 3060.
40 D. K. Cooper, B. Ekser, J. Ramsoondar, C. Phelps and D. Ayares, *J. Pathol.*, 2016, **238**, 288–299.
41 T. H. Kim, J. J. Yan, J. Y. Jang, G. M. Lee, S. K. Lee, B. S. Kim, J. J. Chung, S. H. Kim, Y. Jung and J. Yang, *Sci. Adv.*, 2021, **7**, eabg2237.
42 S. Haykal, N. Barone, S. Rostami, S. Moshkelgosha, S. Juvet, S. Keshavjee and D. Ghazarian, *Plast. reconstr. surg., Glob. open.*, 2023, **11**(3), e4831.
43 R. Edri, I. Gal, N. Noor, T. Harel, S. Fleischer, N. Adadi, O. Green, D. Shabat, L. Heller, A. Shapira, I. Gat-Viks, D. Peer and T. Dvir, *Adv. Mater.*, 2019, **31**, e1803895.
44 L. Xu, Y. Guo, Y. Huang, Y. Xu, Y. Lu and Z. Wang, *J. Biomater. Appl.*, 2019, **33**, 1252–1264.
45 A. M. Padma, L. Carrière, F. Krokström Karlsson, E. Sehic, S. Bandstein, T. T. Tiemann, M. Oltean, M. J. Song, M. Brännström and M. Hellström, *npj Regener. Med.*, 2021, **6**, 26.
46 A. B. Alshaikh, A. M. Padma, M. Dehlin, R. Akouri, M. J. Song, M. Brannstrom and M. Hellstrom, *Reprod. Biol. Endocrinol.*, 2020, **18**, 75.
47 S. D. Sackett, D. M. Tremmel, F. Ma, A. K. Feeney, R. M. Maguire, M. E. Brown, Y. Zhou, X. Li, C. O'Brien, L. Li, W. J. Burlingham and J. S. Odorico, *Sci. Rep.*, 2018, **8**, 10452.
48 C. Yang, N. Chung, C. Song, H. W. Youm, K. Lee and J. R. Lee, *Biofabrication*, 2022, **14**, 011001.
49 H. S. Kong, J. Lee, H. W. Youm, S. K. Kim, J. R. Lee, C. S. Suh and S. H. Kim, *PLoS One*, 2017, **12**, e0184546.